

FULL PAPER

Open Access



Ultra-low velocity zone heterogeneities at the core–mantle boundary from diffracted PKKP_{ab} waves

Xiaolong Ma and Xinlei Sun*

Abstract

Diffracted waves around Earth's core could provide important information of the lowermost mantle that other seismic waves may not. We examined PKKP_{ab} diffraction waves from 52 earthquakes occurring at the western Pacific region and recorded by USArray to probe the velocity structure along the core–mantle boundary (CMB). These diffracted waves emerge at distances up to 10° past the theoretical cutoff epicentral distance and show comparable amplitudes. We measured the ray parameters of PKKP_{ab} diffraction waves by Radon transform analysis that is suitable for large-aperture arrays. These ray parameters show a wide range of values from 4.250 to 4.840 s/deg, suggesting strong lateral heterogeneities in sampling regions at the base of the mantle. We further estimated the P-wave velocity variations by converting these ray parameters and found the CMB regions beneath the northwestern edge of African Anomaly (Ritsma et al. in *Science* 286:1925–1928, 1999) and southern Sumatra Islands exhibit velocity reductions up to 8.5% relative to PREM. We suggest that these low velocity regions are Ultra-low velocity zones, which may be related to partial melt or iron-enriched solids.

Keywords: Diffracted PKKP_{ab} waves, Core–mantle boundary, Lateral heterogeneity, Low velocity zones

Introduction

It is well known that there exist significantly complex structures at the core–mantle boundary (CMB). These complex structures range from large low shear velocity provinces (LLSVPs) of thousands of kilometers (e.g., Ni and Helmberger 2003; Garnero and McNamara 2008; Garnero et al. 2016) to small-scale scatterers of a few to tens of kilometers (e.g., Vidale and Hedlin 1998; Mancinelli and Shearer 2013; Waszek et al. 2015). Other complex features include ultra-low velocity zones (ULVZs) (Helmberger et al. 2000; Rost and Revenaugh 2003a; Rost et al. 2010), D'' discontinuity (e.g., Nataf and Houard 1993; Rost and Revenaugh 2003b; Hernlund et al. 2005) and seismic anisotropy in D'' (e.g., Kendall and Silver 1996; Garnero et al. 2004; Long 2009; Lynner and Long 2014). All these complex structures are not surprising since the CMB is the most dramatic thermal

and compositional boundary within the Earth (Garnero 2000). Although these structures are important for us to understand the dynamic process and evolution inside the Earth (Garnero 2004; McNamara and Zhong 2005; Tackley 2012), due to uneven distribution of earthquakes and seismic stations, there are still areas near the CMB that have not been well probed. Moreover, conventional tomographic methods often poorly resolve small-scale structures at the CMB owing to ray coverage and frequency content (Rawlinson et al. 2010; Liu and Gu 2012). In contrast, unconventional methods, such as diffracted waves traveling a long distance along the CMB, may provide additional information.

Core-diffracted waves, such as P_{diff} and SPdKS/SKPdS waves, have been widely used to probe the lowermost mantle structure (e.g., Wyssession 1996; Earle and Shearer 2001; Thorne and Garnero 2004; Xu and Koper 2009; Thorne et al. 2013; Hosseini and Sigloch 2015). Although their results have revealed strong lateral velocity variations near the CMB, there are limitations in their mapping areas due to small detectable amplitudes or specific

*Correspondence: xsun@gig.ac.cn
State Key Laboratory of Isotope Geochemistry, Guangzhou Institute of Geochemistry, Chinese Academy of Sciences, Wushan, Tianhe, Guangzhou 510640, China

raypath geometry of phases used. As a complementary approach, diffracted PKKP_{ab} waves can sample regions that other phases cannot, thus improving the mapping coverage of small-scale structures at the CMB.

PKKP is a P-wave traveling through the core and reflecting once at the underside of the CMB. Like PKP , there are four branches of PKKP phase (PKKP_{ab} , PKKP_{bc} , PKKP_{cd} and PKKP_{df}) (Fig. 1). In general, PKKP_{cd} and PKKP_{df} are difficult to see due to very small amplitudes, while PKKP_{ab} and PKKP_{bc} are more easily identified in short-period seismograms (Earle 2002; Rost and Garnero 2006; Ivan and Cormier 2011; Niu et al. 2012).

The theoretical cutoff distance of PKKP_{ab} for a 500-km-depth earthquake in the PREM (Dziewonski and Anderson 1981) is about 104° (minor arc distance). However, because PKKP_{ab} waves can diffract around the CMB (Fig. 1), the diffracted waves can always be detected at distances beyond this cutoff distance in short-period seismograms. Although the diffraction could occur on either (or both) side(s) of the PKKP_{ab} raypath along the CMB, in this paper, we name the diffracted waves as PKKP_{ab} diffraction waves.

PKKP_{ab} diffraction waves can be clearly detected at distances beyond this cutoff distance in short-period

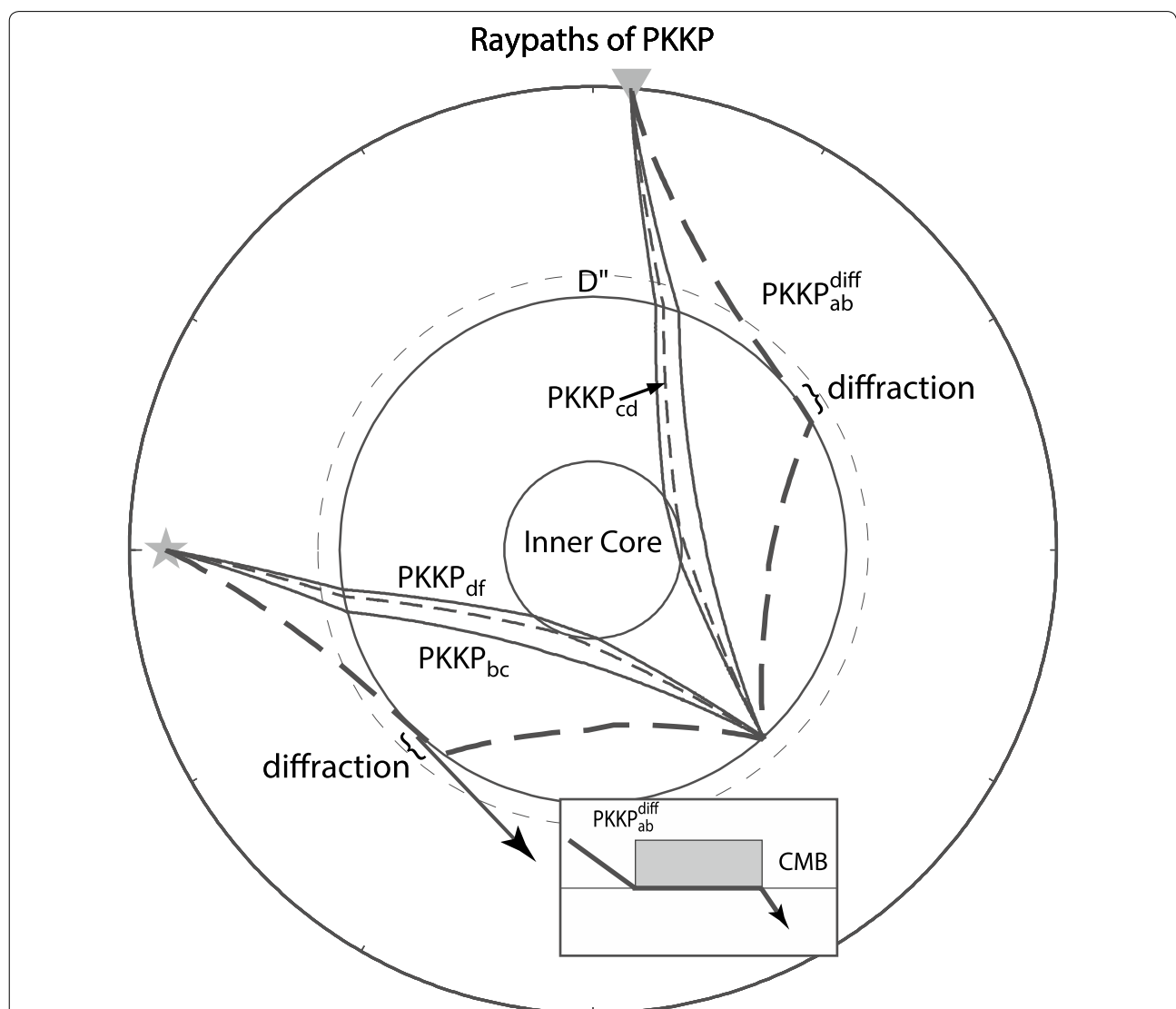


Fig. 1 Raypaths for different PKKP branches. PKKP_{df} and PKKP_{bc} raypaths are denoted as solid lines, and PKKP_{cd} as well as PKKP_{ab} diffraction paths are denoted as thinner and thicker dashed lines, respectively. The ray paths are generated for an event (gray star) with a focal depth of 500 km, and the minor epicenter distance to the station (gray inverted triangle) is 95° . The diffracted portions along the core–mantle boundary on the two sides are about 9.0° in total. The inserted box shows one-sided diffraction of PKKP_{ab} waves along the CMB

seismograms, thus providing unique solutions to small-scale velocity structures at the CMB. In spite of these merits, there are only a few studies utilizing PKKP_{ab} diffraction waves (Rost and Garnero 2006; Ivan and Cormier 2011), which is mainly because of lack of high-quality data. With the increase in temporary/permanent stations all around the world, PKKP_{ab} diffraction phase now may provide more opportunities to resolve the CMB structures in regions that have not been studied previously.

In this study, we collect PKKP_{ab} diffraction waves recorded by the USArray from earthquakes located along the western boundary of Pacific Ocean and try to resolve CMB velocity structures by measuring the ray parameters of these diffracted waves. The wide distribution of USArray ensures broader mapping areas sampled by PKKP_{ab} diffraction waves. This study exhibits a wide range of velocity perturbations from about -8.5 to $+4.2\%$ relative to PREM. The results also show two Ultra-low velocity zones beneath the northwestern edge of African and southern Sumatra Islands, which could be explained by thermal/chemical variations, such as partial melting and iron-enriched material in the lowermost mantle.

Data and methods

In order to obtain clear PKKP_{ab} diffraction phases, and to avoid possible contaminations from depth phases or strong scattering in the lithosphere, we only selected earthquakes with depths greater than 100 km and magnitudes larger than 5.4 (Table 1). We also excluded data with epicentral distances larger than 104° where PKKP_{ab} waves begin to appear. Therefore, our earthquakes are generally distributed along the western boundary of Pacific Ocean (Fig. 2). All the stations we selected are from USArray, which spans a large area with a relatively dense distribution. After removing the instrument response and band-pass filtering with a frequency band of 0.9–2.1 Hz, we visually checked the seismic recordings and selected the ones with clear PKKP_{ab} diffraction phases and good signal-to-noise ratios. During this process, the recordings with very complex waveforms are also discarded, to avoid possible biases from complicate rupture process in the source. Finally, a total of 2540 seismic recordings from 52 earthquakes are selected. Two examples of such PKKP waves are shown in Fig. 3.

To estimate seismic velocities of the lowermost mantle, we first determined the ray parameters of the PKKP_{ab} diffraction waves. Then, we converted the obtained ray parameters into apparent velocities according to:

$$V_{\text{cmb}} = R_{\text{cmb}}/p \quad (1)$$

Table 1 Earthquakes used in this study

No.	Date	Latitude	Longitude	Depth	Mag (Mw)
1	2006.12.27.20.42	-11.4345	166.4710	137.5	6.0
2	2007.11.19.01.18	-13.5186	166.9850	124.7	6.3
3	2008.09.08.18.52	-13.6631	167.0310	118.4	6.9
4	2009.03.26.19.19	-18.0120	-178.4360	577.4	5.9
5	2009.09.03.13.26	19.3514	144.7600	446.9	6.2
6	2009.10.25.07.53	-20.4310	-176.2160	231.3	6.0
7	2009.10.31.19.09	-20.8720	-178.5080	536.9	5.9
8	2010.03.04.14.02	-21.2118	-178.6730	558.9	6.5
9	2010.03.08.09.47	-23.0250	-177.1090	171.4	6.1
10	2010.03.20.14.00	-23.0354	-179.1010	413.0	6.6
11	2010.06.17.13.06	-23.1320	-177.2220	155.5	6.0
12	2010.06.30.04.31	-23.2850	179.1800	572.8	6.4
13	2010.08.04.07.15	-23.5142	-179.7430	562.3	6.5
14	2010.08.15.15.09	-26.0435	178.4770	551.8	6.3
15	2010.12.13.01.14	26.9670	140.0160	524.5	6.2
16	2011.01.12.21.32	27.2502	125.7230	228.2	6.5
17	2011.01.23.19.15	27.4033	126.8230	152.0	5.8
18	2011.02.21.10.57	29.0570	139.2510	436.0	6.5
19	2011.08.25.10.39	29.9330	138.8870	421.9	5.9
20	2011.11.08.02.59	31.1797	130.1830	167.2	6.9
21	2012.02.10.01.47	-33.1905	179.7820	211.2	6.0
22	2012.07.18.08.09	-3.3752	152.2790	418.9	5.9
23	2012.10.23.08.53	-33.8530	179.4020	195.0	5.9
24	2013.04.05.13.00	42.7130	131.1050	561.9	6.3
25	2013.04.21.03.22	-5.5179	146.8590	219.7	6.1
26	2013.05.23.17.19	-5.7808	154.4580	353.5	7.4
27	2013.06.15.11.20	-5.7825	148.3750	180.8	6.0
28	2013.07.24.03.32	-23.132	-177.2220	155.5	6.0
29	2014.03.02.20.11	27.4312	127.3670	119.0	6.5
30	2014.03.05.09.56	-14.7378	169.8230	638.0	6.3
31	2014.05.04.09.15	-24.6108	179.0860	527.0	6.6
32	2014.05.09.10.32	-18.9616	-175.5360	192.3	5.9
33	2014.06.30.19.55	28.3404	138.8440	511.0	6.2
34	2014.07.21.14.54	-19.8015	-178.4000	615.4	6.9
35	2014.11.01.18.57	-19.6903	-177.7590	434.0	7.1
36	2014.12.30.21.17	-20.3263	-178.5640	599.3	6.0
37	2015.03.16.03.00	-4.0737	152.0290	196.0	5.9
38	2015.04.28.16.39	-20.8865	-178.6330	581.0	6.1
39	2015.05.20.00.30	-19.3021	-175.5250	203.0	6.0
40	2015.06.16.06.17	-20.3944	-179.0020	656.0	5.9
41	2015.06.21.21.28	-20.4307	-178.3280	562.6	6.0
42	2015.06.23.08.59	-19.5686	-175.0400	138.0	5.5
43	2015.06.23.12.18	27.7375	139.7250	460.0	6.5
44	2015.07.07.20.03	-22.9379	-177.1330	169.6	5.8
45	2015.07.17.18.49	-18.1214	-178.1890	536.1	5.8
46	2015.11.02.03.04	-18.1736	-177.8380	608.4	5.6
47	2016.02.14.18.09	30.3018	138.8500	412.8	5.7
48	2016.05.27.04.08	-20.8101	-178.6480	567.5	6.4
49	2016.05.28.05.38	-21.9724	-178.2040	405.7	6.9

Table 1 continued

No.	Date	Latitude	Longitude	Depth	Mag (Mw)
50	2016.08.22.09.33	29.8965	139.1310	404.4	5.6
51	2016.08.25.17.04	30.6151	137.8460	456.0	5.9
52	2016.09.24.21.28	-19.7819	-178.2440	596.4	6.9

where V_{cmb} is the apparent velocity of the CMB, p is the ray parameter of PKKP_{ab} diffraction wave and R_{cmb} is the radius of the core in the Earth.

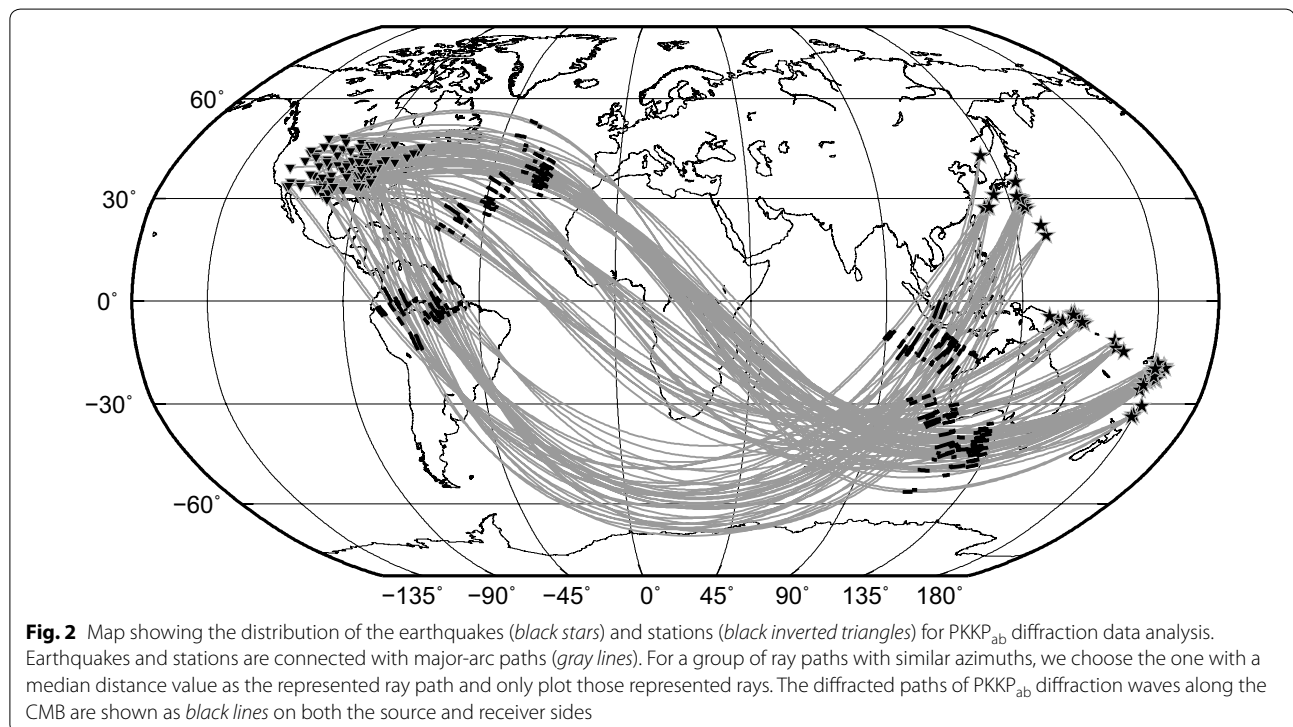
Considering the complex waveforms and the large apertures of the USArray, instead of using traditional methods such as beam forming or slant stacking (Rost and Thomas 2002), we adopted an alternative approach, the Radon transform method (we termed it as RTM hereafter) (Gu and Sacchi 2009; Schultz and Gu 2013), to calculate the ray parameters of PKKP_{ab} diffraction waves. Radon transform is defined as:

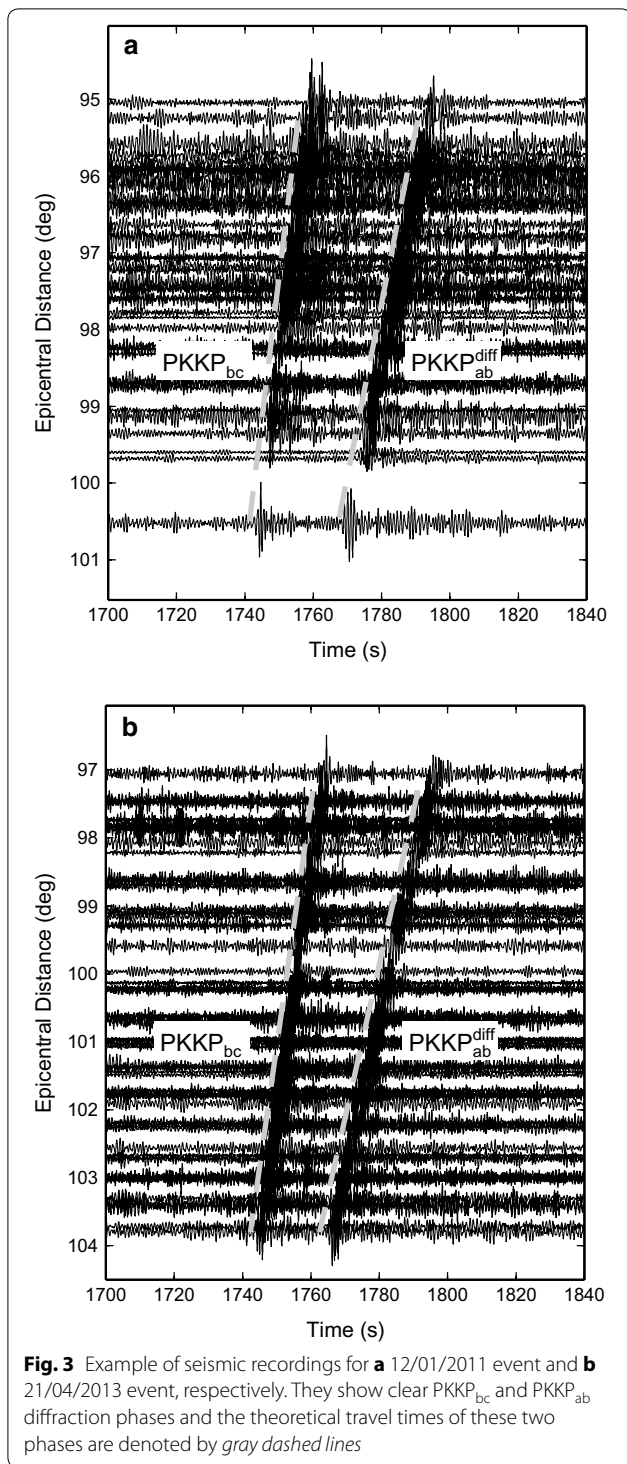
$$m(\tau, p) = \sum_{i=1}^N d(t = \varphi(\tau, \Delta, p), \Delta_i)$$

where φ is a time function that depends on reduced time τ , epicenter Δ and ray parameter p . In this study, we assumed a linear relationship with $\varphi(\tau, \Delta, p) = \tau + p\Delta$ for the analysis of PKKP_{ab} diffraction wave owing to its geometric propagation path inside the Earth. RTM first transforms the data from $t - \Delta$ domain into $\tau - p$

domain and filters the transformed data in order to discriminate different ray parameters by inversion [details can be found in Gu and Sacchi (2009)]. The strongest energy focus in Radon (τ, p) domain corresponds to the expected ray parameter along which the data are stacked. The obvious advantage of RTM is that it could isolate the ray parameter based on inversion in $\tau - p$ domain, which is suggested to be more robust and reliable (Beylkin 1987; Sacchi and Ulrych 1995). Besides, this method could apply to a wider range of epicenter distances and is more efficient to phases whose ray parameters are very close than conventional stacking methods (Schultz and Gu 2013).

Before we use RTM, several procedures are carried out to ensure data quality and to reduce contaminations from heterogeneous structures in the mantle. Firstly, we calculated the amplitude envelope of all the seismograms. This procedure simplifies the complicated short-period waveforms without loss of general information (Eaton and Kendall 2006; Gu and Sacchi 2009), thus making it easier to handle. Then, we corrected ellipticity (Dziewonski and Gilbert 1976; Kennett and Gudmundsson 1996) and mantle heterogeneity through GyPSuM tomographic model (Simmons et al. 2010). Finally, we classified all the recorded data into different groups for every 5° according to their azimuths. Considering that the sampling regions of our data span about 30° in longitude and 75° in latitude at the CMB, this classification ensures that for each event, seismograms in the same group are aligned in almost the





same great circle, thus avoiding azimuthal heterogeneity in the source and receiver regions. After grouping by azimuth, we further checked the number and distribution of the data in each subgroup and excluded the subgroups that have less than 10 seismic recordings and

unevenly distributed data in distance, in order to avoid possible bias from individual anomalous PKKP_{ab} diffraction waves. After this selection, in total, we obtained 106 event–station subgroups (gray lines in Fig. 2). In the next step, RTM is applied to each subgroup separately to obtain ray parameters. Then, we converted all the ray parameters into P-wave velocities based on Eq. (1).

The obtained apparent velocity from ray parameter depends on the frequency of the waves and the velocity structures at the base of the mantle (Chapman and Phinney 1972; Mula and Müller 1980). Therefore, the apparent velocity in Eq. (1) is different from the actual velocity at the CMB (Mula and Müller 1980). However, in our study, the estimated sampling thickness for short-period PKKP waveforms is about one or two wavelength, which is on the order of tens of km above the CMB (Sylvander et al. 1997). Thus, the inferred apparent velocity is a good approximation of the actual velocity near the CMB.

Results

First, synthetic tests are carried out to validate the RTM we adopted. Considering our data are not sensitive to discontinuities (no top reflections at a discontinuity are observed) and the results are averaged velocities above the CMB, we tested two models modified from PREM, in which it has either a gradual P-wave velocity decrease from 0 to 8% (low velocity model) or increase from 0 to 6% (high-velocity model) in a 60-km layer atop the CMB (Fig. 4a). The choice of 60 km is because of its consistency with the thickness of general ULVZs and the resolution of our PKKP diffractions. Synthetic seismograms for a 500-km-deep earthquake are calculated using DSM (direct solution method) (Geller and Takeuchi 1995; Kawai et al. 2006) (Fig. 4b). The retrieved slownesses for the low velocity and high velocity models generally represent their characteristics of velocity change. Here we only show results from the low velocity model (Fig. 4b). It is obvious that the PKKP_{ab} diffraction phases appear in the epicentral distances much shorter than its theoretical cutoff distance. The restored ray parameter for these synthetic seismograms from RTM is 4.520 s/deg, which is larger than that of PREM (4.428 s/deg) (Fig. 4c). The converted velocity according to Eq. (1) is ~2% slower than that of PREM. The recovered velocity from the high-velocity model is about +2.6%. Although the synthetic tests do not fully recover the averaged velocity changes in the input model (-4 and 3%), it is not surprising, considering the non-ray theoretical nature and finite-frequency effects of diffracted waves (Hosseini and Sigloch 2015). We then applied RTM to calculate the PKKP ray parameters for each subgroup of seismograms in our data. As an example, Fig. 5 exhibits the results of data in Fig. 3.

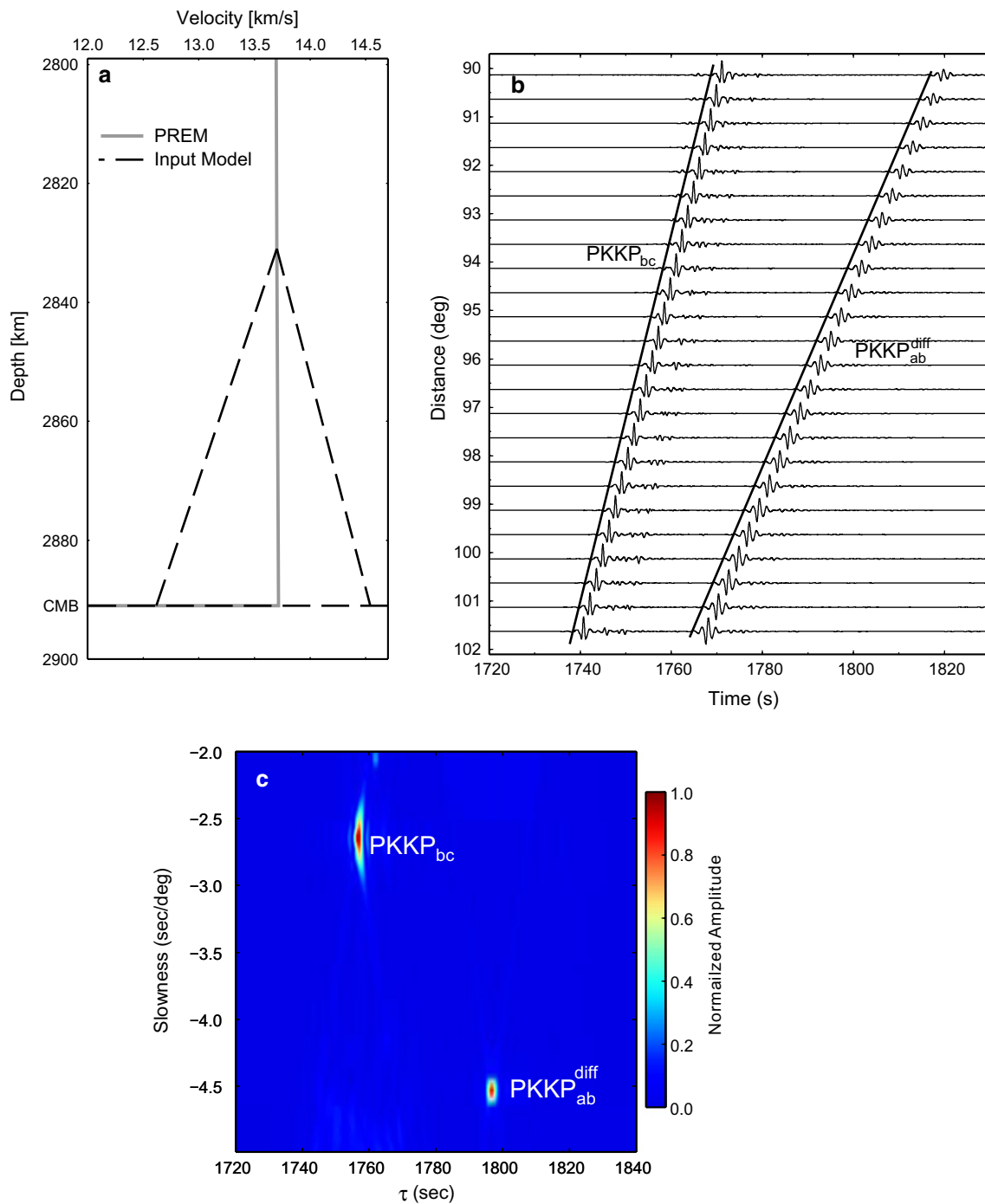
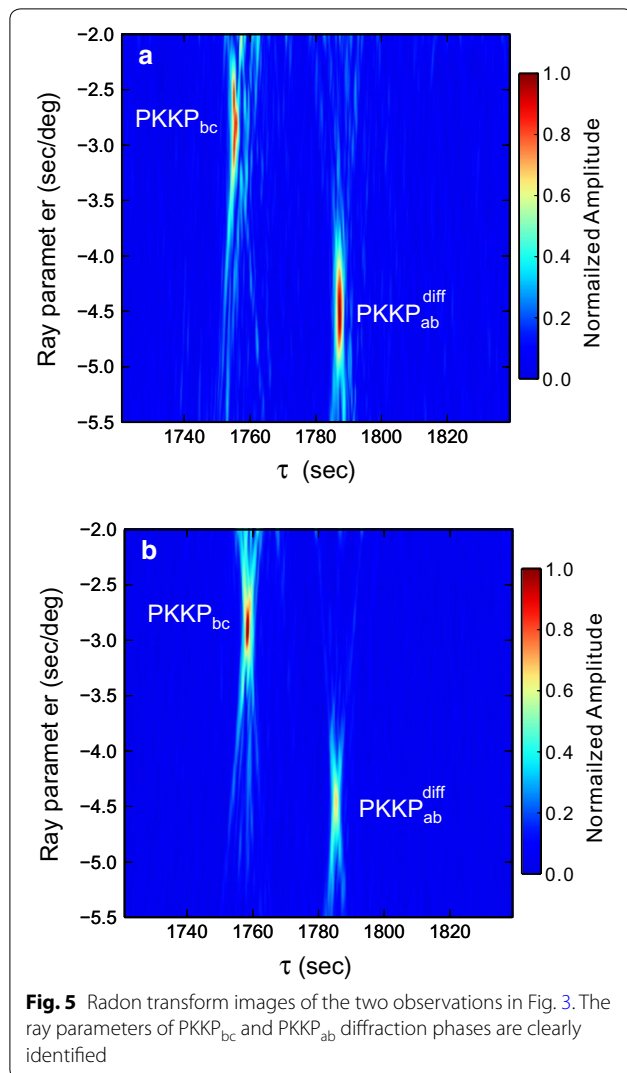


Fig. 4 **a** Models used in synthetic tests of RMT. Compared to PREM (gray line), the test model (black line) has either a P-wave velocity decrease from 0 to 8% (low velocity model) or an increase from 0 to 6% (high-velocity model) in a 60-km layer atop the CMB. **b** Synthetic seismograms calculated using DSM for a 500-km-depth event based on the low velocity model in **a**. The seismograms are band-pass filtered with the same frequency band as the observed data. The black lines denote the travel times of PKKP_{bc} and PKKP_{ab} diffraction waves, respectively. **c** Radon transform image of synthetic seismograms in **b**. The normalized amplitudes (shown in different color) are energy of seismogram summations along their corresponding ray parameters



The ray parameters of both PKKP phases can be identified very clearly.

Most of the PKKP_{ab} diffractions can only be seen clearly in frequency bands between 0.5 and 2.1 Hz. To check the frequency effect on the velocity of PKKP_{ab} diffraction, we choose several frequency bands and calculated their ray parameters separately. Figure 6 shows the histograms of ray parameters of PKKP_{ab} diffraction waves in three different frequency bands (0.9–2.1, 0.5–1.5 and 0.5–2.1 Hz). The mean values of the ray parameter are 4.506, 4.517 and 4.503 s/deg, with standard deviations of 0.113, 0.093 and 0.114 s/deg, respectively. Similar results in different frequency bands suggest that velocity structures at the top of several tens of km above the CMB in this area are quite uniform.

The variations of the ray parameter are not from structures near the source/receiver, since the aperture of the stations and the earthquakes would average the

difference effectively. The tomographic corrections for PKKP_{ab} diffraction waves in the mantle are also rather small, indicating that the heterogeneity in the mantle may not be the cause either. It is also suggested that noise in the data or CMB topography could not account for such various and coherent ray parameter variations of PKKP_{ab} diffraction waves (Sylvander et al. 1997; Doornbos 1980). Based on these evidences, we suggest that the variations in ray parameter should be from the complex structures along the CMB.

The converted velocity variations from ray parameters are plotted on the middle points of the diffracted paths along the CMB on both sides, with a P-wave tomographic model of mantle from GyPSuM (Simmons et al. 2010) as background (Fig. 7). The areas sampled by PKKP_{ab} diffraction waves in this study are generally located along two “strips” at the CMB. On the source side, the sampled region starts from the southwest of Indonesia, extends across the southwest of Australia and ends up at southern Indian Ocean. On the receiver side, the region starts from the northeast side of South America, extends across the Atlantic Ocean and then ends at the northern part of Atlantic Ocean. Most of the sampled regions exhibit low velocity anomalies in the tomographic image, except for only a few high-velocity areas.

Discussion

ULVZs at the CMB

The inferred P-wave velocity perturbations along the CMB from PKKP_{ab} diffraction waves exhibit a wide range, and show velocity reductions up to about 8.5%. We approximately divided the diffracted regions at the CMB into four regions, with two on the receiver side and their corresponding regions on the source side (as labeled in Fig. 7). In comparison with tomographic model of GyPSuM, we found that the north region on the receiver side is located at the northwestern edge of African Anomaly (Ni and Helmberger 2003; Wang and Wen 2004, 2007; Sun and Miller 2013). Its corresponding region on the source side is in the southwest of Australia. The low velocity variations in these regions could be between –6.0 and –8.5%, which is quite similar to that of ULVZs. Since the southwest of Australia is a region with no low velocity signature or a low possibility of ULVZs (Thorne and Garnero 2004; Lay 2015), we suggest that the resulted *P* velocity heterogeneities are from the receiver side, the northwestern edge of African Anomaly.

Our results show an overall change of the velocity reduction from east to west in this region (Fig. 8), with the strongest velocity reduction (~8.5%) in the eastern part (near the northwestern edge of African Anomaly). We binned the P-wave velocity reductions using a 10-degree moving window with a 5-degree overlap.

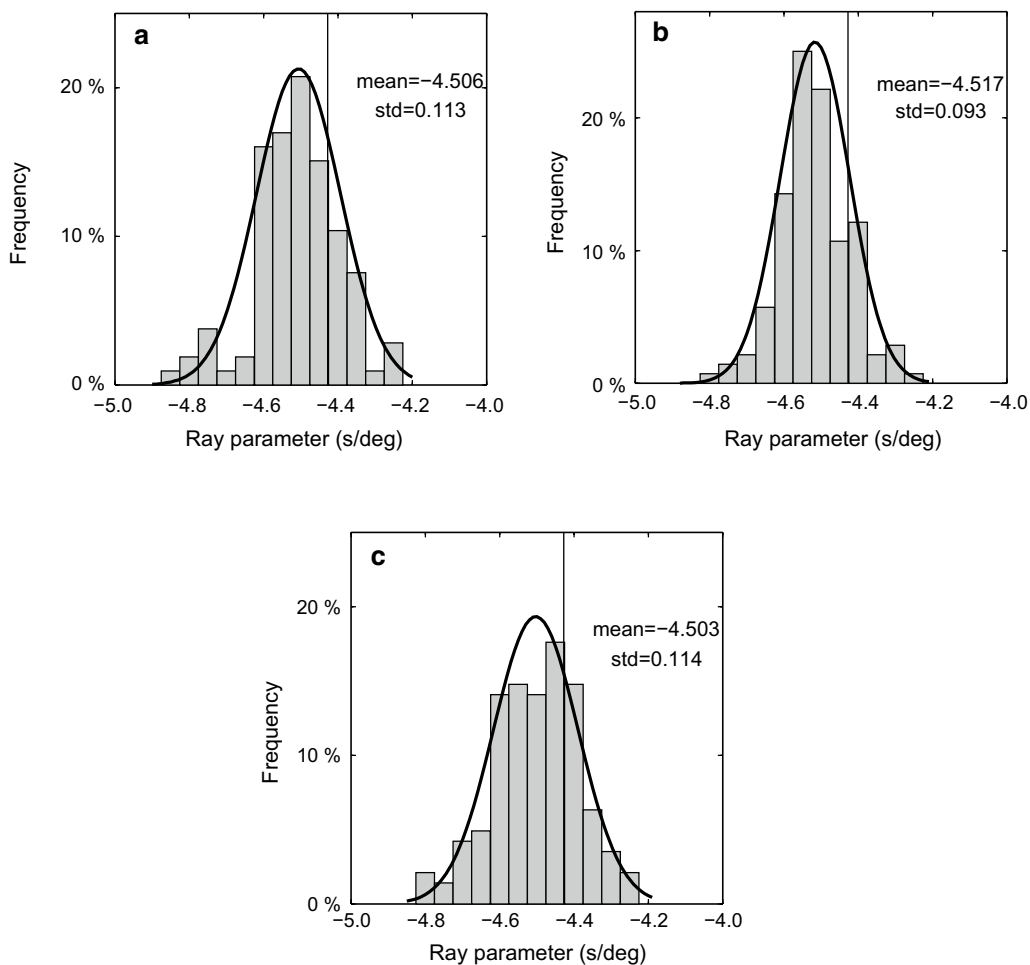


Fig. 6 **a** Histogram of PKKP_{ab} diffraction ray parameters after ellipticity and mantle heterogeneity corrections. The seismograms are band-pass filtered between 0.9 and 2.1 Hz. The mean value of the ray parameters is 4.506 s/deg, and the standard deviation is 0.113 s/deg. The vertical black line denotes the theoretical ray parameter of PKKP_{ab} diffraction calculated for PREM. **b, c** same as **a**, but for the ray parameter distribution of PKKP_{ab} diffractions from 0.5–1.5 Hz and 0.5–2.1 Hz bands, respectively

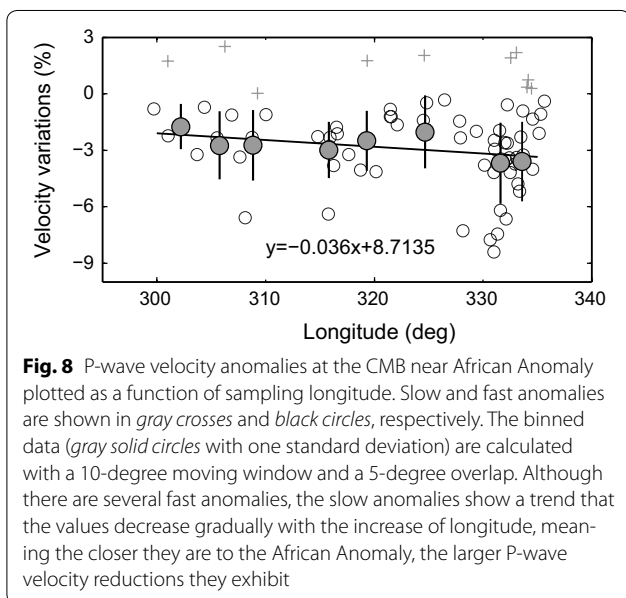
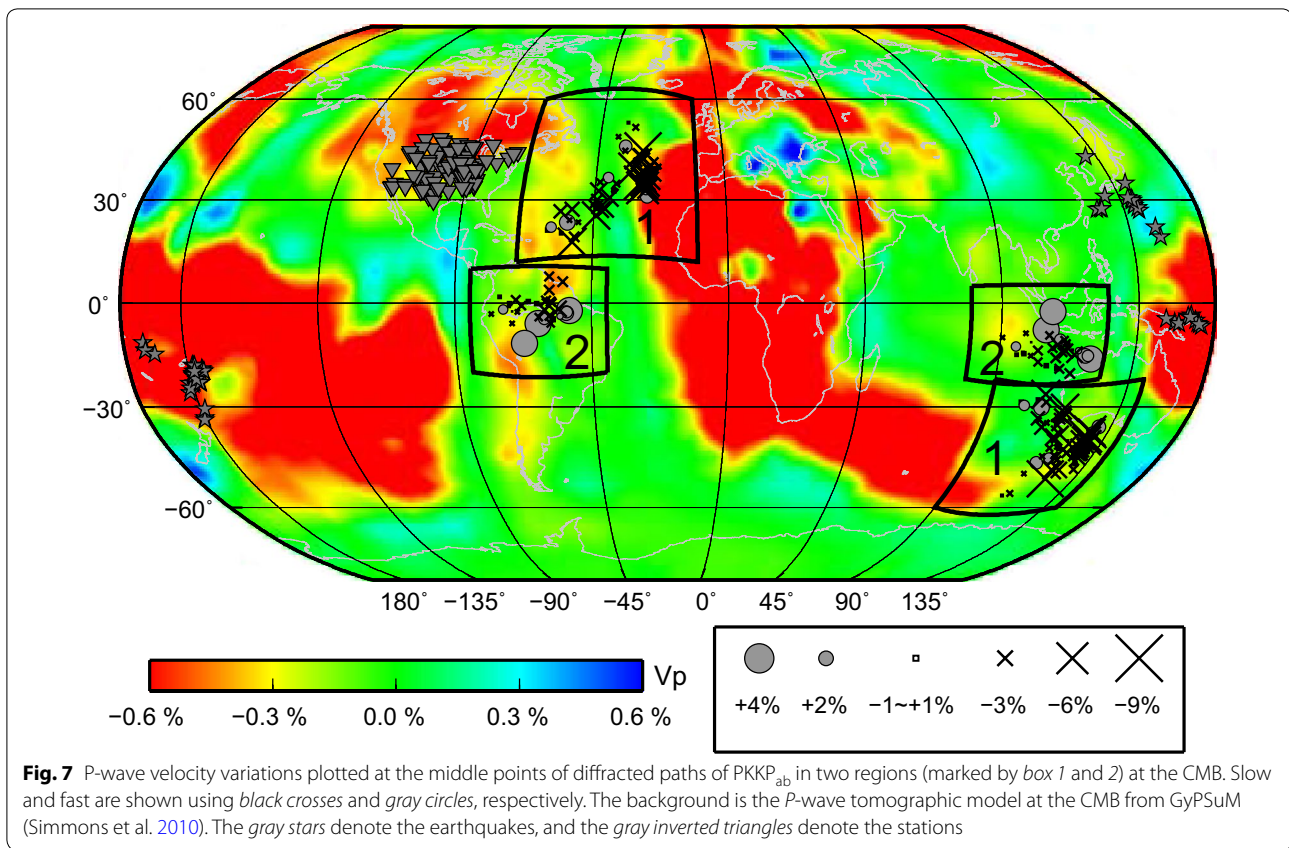
There is an overall trend that the slow anomalies decrease gradually with the increase in longitude, although it is not very strong. This may indicate that ULVZs are closely related to the boundary of LLSVP (Thorne et al. 2004; McNamara et al. 2010; Hier-Majumber and Drombosky 2016), and the velocity reduction in ULVZ may also be associated with its distance to LLSVP. Further investigations with more data may be needed.

Thorne and Garnero (2004) have systematically studied the global SPdKS waves and proposed a ULVZ likelihood map. Our region in the northwestern side of African Anomaly in general agrees with the region of high ULVZ likelihood in their map, but extends further west. Using PKKP data recorded by Yellowknife array, Rost and Garnero (2006) also mapped ULVZs in a region located further north of our study region, with a similar lateral extension. Their results did not show systematic velocity

changes, but they did notice that PKKP_{ab} diffraction waves sampling the west of the region show larger departures from theoretical ray paths than those to the east.

Some low velocity zones with velocity reductions of 3–5% are also detected on the source side beneath southern Sumatra Islands. Their corresponding regions on the receiver side are in the northeast of South America. South America is a region that generally shows high-velocity anomalies in various tomographic models (Zhao 2004; Li et al. 2008; Simmons et al. 2010) and shows low likelihood in SPdKS study (Thorne and Garnero 2004). Therefore, this region is unlikely to cause the low velocities we observed. In other words, the velocity reductions in region 2 more likely result from the CMB beneath southern Sumatra Islands.

The high-velocity anomalies (up to 4%) in region 2 are more likely to be related to subducted slabs, thus making



we cannot definitely rule out the contribution from this region either. In this case, we could not clearly solve the origin ambiguity of PKKP_{ab} diffraction anomalies, although South America could provide a more proper explanation. It is noted that the high-velocity anomalies could not merely result from the temperature change, because such change would be too much under the CMB conditions (Wentzcovitch et al. 2006). We suggest that chemical changes in the subducted oceanic crust may also play an important role in this case.

In general, our results show strong lateral velocity variations that can change between -8.5% and up to $+4.2\%$, which is consistent with the magnitude of velocity perturbations from both global (e.g., Sylvander et al. 1997) and regional studies (e.g., Xu and Koper 2009). These strong lateral heterogeneities are much larger than those calculated from global tomographic models and imply significantly complex structures at the CMB that have long been known to exist [see Garnero (2000); Lay and Garnero (2011) for a review], even on the small-scale level (Ma et al. 2016; Sun et al. 2016). The explanations for these heterogeneities, however, are still inconclusive. Wyssession et al. (1992) correlated the strong lateral heterogeneity at the CMB with core flow models from geomagnetics (Voorhies 1986). They demonstrated that the

the north of South America a good place for these heterogeneities. However, in the corresponding source side beneath southern Sumatra Islands, the high velocities are located on both sides of the slow anomaly, which

adjacent fast and slow regions possibly correspond to areas of core upwelling and down welling, respectively. Other explanations probably include chemical variations and/or thermal variations [see Tackley (2012) for a review]. For the origin of ULVZ-like structures, partial melt (Williams and Garnero 1996; Berryman 2000; Lay et al. 2004; Hernlund and Tackley 2007) or iron-enriched lower mantle materials introduced by subducted paleo-slabs (Dobson and Brodholt 2005) or core interactions from below (Sakai et al. 2006) may provide reasonable explanations (Wicks et al. 2010; Bower et al. 2011).

Comparison with previous studies

Unlike previous studies (Rost and Garnero 2006), in this study, we did not carry out the analysis of absolute travel times of PKKP_{ab} diffraction or relative travel times with respect to PKKP_{bc}. Travel time analysis, though, could verify our results inferred from ray parameters. However, in the short-period (0.5–2.0 s) recordings, both PKKP_{ab} diffraction waves and PKKP_{bc} waves are strongly affected by the high-frequency coda waves from scattering in the lithosphere, making it difficult to pick their onsets. In contrast, ray parameter analysis is less biased by small-scale inhomogeneities near the source and along the descending legs of the ray as long as the receivers are aligned closely in great circle paths (Ivan et al. 2015).

Global/regional studies of P_{diff} (e.g., Wysession and Okal 1989; Wysession et al. 1992; Sylvander et al. 1997; Ivan et al. 2015) generally determine ray parameters based on equation $p = dT/d\Delta$, where T is the travel time of a target phase and Δ is the epicentral distance. For dense seismic arrays, beam forming or slant stacking (Rost and Thomas 2002) is often used, assuming incoming waves are plane waves. However, in our study, the onsets of PKKP_{ab} diffraction waves are hard to recognize in high-frequency waveforms; thus, the first method is not suitable. On the other hand, the distance of our data spans about 10°, so beam forming or slant stacking method is not proper either (Thomas et al. 1999). The RTM we adopted in this study could isolate different ray parameters by inversion in $\tau - p$ domain, which not only fits the data globally, but also can effectively isolate similar ray parameters with less uncertainty. Although the RTM has been used previously in mid-mantle studies (e.g., An et al. 2007; Gu et al. 2009), this is the first time we successfully apply it to PKKP signals of a large distance range.

In general, PKKP_{ab} diffractions have no power to resolve the ambiguity of CMB heterogeneity locations. To resolve this problem, one way is to compare with other phases that sample similar regions, at least in one side, such as PcP, ScP, SPdKS and PKP (e.g., Idehara 2011; Jensen et al. 2013; Ma et al. 2016). In most cases, this may

be difficult to do because of limited earthquake and station distributions. Then, the much easier way is to compare with mantle tomographic models, since small-scale structures are usually related to large-scale heterogeneities as indicated in tomography models (Zhao 2004; Montelli et al. 2006; French and Romanowicz 2015). Nevertheless, more characteristics of PKKP waves may be needed to identify anomaly locations.

Conclusions

We have examined diffracted PKKP_{ab} waves from 52 earthquakes occurring along the boundary of Western Pacific and recorded by USArray. Ray parameters of PKKP_{ab} diffraction waves are determined using the Radon transform method and then converted to velocity variations in the sampling regions at the base of the mantle. Our results show that beneath the northwestern edge of African Anomaly and southern Sumatra Island, the velocity reductions are as large as about –8.5%, which suggests the existence of ULVZs. The velocity change in northern Atlantic Ocean may indicate different effects that LLSVP plays on ULVZs according to the distance away from it. It should be also noted that although PKKP_{ab} diffractions enable us to resolve small-scale structures at the CMB and improve the sampling coverage, intrinsic ambiguity exists in identifying the exact areas of velocity anomaly. More evidences from tomographic models and additional phases such as SPdKS and ScP are needed to solve this problem in the future.

Abbreviations

CMB: Core–mantle boundary; LLSVPs: Large low shear velocity provinces; LVZ: Low velocity zone; PREM: Preliminary reference Earth model; RTM: Radon transform method; ULVZs: Ultra-low velocity zones.

Authors' contributions

XM and XS carried out the research. XM analyzed the seismic data. XM and XS wrote the manuscript. Both authors read and approved the final manuscript.

Acknowledgements

We thank Azusa Nishizawa and three anonymous reviewers for their constructive comments and suggestions. The manuscript benefits a lot from them. The authors are supported by China National Science Foundation (No. 41330209) and the 973 project of Ministry of Science and Technology of China (2014CB845901). Figures are made using Generic Mapping Tools (Wessel and Smith 1995). The facilities of IRIS Data Services, and specifically the IRIS Data Management Center, were used for access to waveforms, related metadata, and/or derived products used in this study. IRIS Data Services are funded through the Seismological Facilities for the Advancement of Geoscience and EarthScope (SAGE) Proposal of the National Science Foundation under Cooperative Agreement EAR-1261681.

Competing interests

The authors declare that they have no competing interests.

Publisher's Note

Springer Nature remains neutral with regard to jurisdictional claims in published maps and institutional affiliations.

Received: 17 January 2017 Accepted: 31 July 2017

Published online: 16 August 2017

References

- An Y, Gu YJ, Sacchi M (2007) Imaging mantle discontinuities using least-squares Radon transform. *J Geophys Res* 112:B10303
- Berryman JG (2000) Seismic velocity decrement ratios for regions of partial melt in the lower mantle. *Geophys Res Lett* 27:421–424
- Beylkin G (1987) Discrete Radon transform. *IEEE Trans Acoust Speech Signal Process* 35:162–172
- Bower DJ, Wicks JK, Gurnis M, Jackson JM (2011) A geodynamic and mineral physics model of a solid-state ultralow-velocity zones. *Earth Planet Sci Lett* 303:193–202
- Chapman DH, Phinney RA (1972) Diffracted seismic signals and their numerical solutions. *Methods Comput Phys* 12:165–230
- Dobson DP, Brodholt JP (2005) Subducted banded iron formations as a source of ultralow-velocity zones at the core-mantle boundary. *Nature* 434:371–374
- Doornbos DJ (1980) The effect of a rough core-mantle boundary on PKKP. *Phys Earth Planet Inter* 21:351–358
- Dziewonski AM, Anderson DL (1981) Preliminary reference Earth model (PREM). *Phys Earth Planet Inter* 25:297–356
- Dziewonski AM, Gilbert F (1976) The Effect of small, aspherical perturbations on travel times and a re-examination of the corrections for ellipticity. *Geophys J Int* 44:7–17
- Earle PS (2002) Origins of high-frequency scattered waves near PKKP from large aperture seismic array data. *Bull Seismol Soc Am* 92:751–760
- Earle PS, Shearer PM (2001) Distribution of fine-scale mantle heterogeneity from observations of Pdiff coda. *Bull Seismol Soc Am* 91:1875–1881
- Eaton DW, Kendall JM (2006) Improving seismic resolution of outermost core structure by multichannel analysis and deconvolution of broadband SmKS phases. *Phys Earth Planet Inter* 155:104–119
- French SW, Romanowicz B (2015) Broad plumes rooted at the base of the Earth's mantle beneath major hotspots. *Nature* 525:95–99
- Garnero EJ (2000) Heterogeneities of the lowermost mantle. *Annu Rev Earth Planet Sci* 28:509–537
- Garnero EJ (2004) A new paradigm for Earth's core-mantle boundary. *Science* 304:834–836
- Garnero EJ, McNamara AK (2008) Structure and dynamics of Earth's lower mantle. *Science* 320:626–628
- Garnero EJ, Maupin V, Lay T, Fouch MJ (2004) Variable azimuthal anisotropy in Earth's lowermost mantle. *Science* 306:259–261
- Garnero EJ, McNamara AK, Shim S-H (2016) Continent-sized anomalous zones with low seismic velocity at the base of Earth's mantle. *Nat Geosci* 9:481–489
- Geller RJ, Takeuchi N (1995) A new method for computing highly accurate DSM synthetic seismograms. *Geophys J Int* 123:449–470
- Gu YJ, Sacchi M (2009) Radon transform methods and their applications in mapping mantle reflectivity structure. *Surv Geophys* 30:327–354
- Gu YJ, An Y, Sacchi M, Schultz R, Ritsema J (2009) Mantle reflectivity structure beneath oceanic hotspots. *Geophys J Int* 178:1456–1472
- HelMBERGER DV, Ni S, Wen L, Ritsema J (2000) Seismic evidence for ULVZ beneath Africa and eastern Atlantic. *J Geophys Res* 105:23865–23878
- Hernlund JW, Tackley PJ (2007) Some dynamical consequences of partial melting in Earth's deep mantle. *Phys Earth Planet Inter* 162:149–163
- Hernlund JW, Thomas C, Tackley PJ (2005) A doubling of the post-perovskite phase boundary and structure of the Earth's lowermost mantle. *Nature* 434:882–886
- Hier-Majumder S, Drombosky TW (2016) Coupled flow and anisotropy in the ultralow velocity Zones. *Earth Planet Sci Lett* 450:274–282
- Hosseini K, Sigloch K (2015) Multifrequency measurements of core-diffracted P waves (Pdiff) for global waveform tomography. *Geophys J Int* 203:506–521
- Idehara K (2011) Structural heterogeneity of an ultra-low-velocity zone beneath the Philippine Islands: implications for core-mantle chemical interactions induced by massive partial melting at the bottom of the mantle. *Phys Earth Planet Inter* 184:80–90
- Ivan M, Cormier VF (2011) High frequency PKKP_{bc} around 2.5 Hz recorded globally. *Pure appl Geophys* 168:1759–1768
- Ivan M, Ghica DV, Gosar A, Hatzidimitriou P, Hofstetter R, Polat G, Wang R (2015) Lowermost mantle velocity estimations beneath the central North Atlantic area from Pdiff observed at Balkan, East Mediterranean, and American stations. *Pure Appl Geophys* 172:283–293
- Jensen KJ, Thorne MS, Rost S (2013) SPdKS analysis of ultralow-velocity zones beneath the western Pacific. *Geophys Res Lett* 40:4574–4578
- Kawai K, Takeuchi N, Geller RJ (2006) Complete synthetic seismograms up to 2 Hz for transversely isotropic spherically symmetric media. *Geophys J Int* 164:411–424
- Kendall JM, Silver PG (1996) Constraints from seismic anisotropy on the nature of the lowermost mantle. *Nature* 381:409–412
- Kennett BLN, Gudmundsson O (1996) Ellipticity corrections for seismic phases. *Geophys J Int* 127:40–48
- Lay T (2015) Deep earth structure: lower mantle and D. *Seismology and the structure of the earth*. In: Kanamori H, Schubert G (eds) *Treatise on geophysics*, vol 1, 2nd edn. Elsevier, Amsterdam, pp 683–723
- Lay T, Garnero EJ (2011) Deep mantle seismic modeling and imaging. *Annu Rev Earth Planet Sci* 39:91–123
- Lay T, Garnero EJ, Williams Q (2004) Partial melting in a thermochemical boundary layer at the base of the mantle. *Phys Earth Planet Inter* 146:441–467
- Li C, van der Hilst RD, Engdahl ER, Burdick S (2008) A new global model for P-wave speed variations in Earth's mantle. *Geochem Geophys Geosyst* 9:Q05018
- Liu Q, Gu YJ (2012) Seismic imaging: from classical to adjoint tomography. *Tectonophysics* 566–567:31–66
- Long MD (2009) Complex anisotropy in D'' beneath the eastern Pacific from SKS-SKKS splitting discrepancies. *Earth Planet Sci Lett* 283:181–189
- Lynner C, Long MD (2014) Lowermost mantle anisotropy and deformation along the boundary of the African LLSVP. *Geophys Res Lett* 41:3447–3454
- Ma X, Sun X, Wiens DA, Wen L, Nyblade A, Anandakrishnan S, Aster R, Huerta A, Wilson T (2016) Strong seismic scatterers near the core-mantle boundary north of the Pacific Anomaly. *Phys Earth Planet Inter* 253:21–30
- Mancinelli NJ, Shearer PM (2013) Reconciling discrepancies among estimates of small-scale mantle heterogeneity from PKP precursors. *Geophys J Int* 195:1721–1729
- McNamara AK, Zhong S (2005) Thermochemical piles beneath Africa and the Pacific. *Nature* 437:1136–1139
- McNamara AK, Garnero EJ, Rost S (2010) Tracking deep mantle reservoirs with ultra-low velocity zones. *Earth Planet Sci Lett* 299:1–9
- Montelli R, Nolet G, Dahlen FA (2006) A catalogue of deep mantle plumes: new results from finite frequency tomography. *Geochem Geophys Geosyst* 7:Q11007
- Mula AH, Müller G (1980) Ray parameters of diffracted long period P and S waves and the velocity and Q structure at the base of the mantle. *J Geophys Res* 86:4999–5011
- Nataf H-C, Houard S (1993) Seismic discontinuity at the top of D'': A world-wide feature? *Geophys Res Lett* 20:2371–2374
- Ni S, HelMBERGER DV (2003) Seismological constraints on the South African superplume: could be the oldest distinct structure on Earth. *Earth Planet Sci Lett* 206:119–131
- Niu F, Kelly C, Huang J (2012) Constraints on rigid zones and other distinct layers at the top of the outer core using CMB underside reflected PKKP waves. *Earthq Sci* 25:17–24
- Rawlinson N, Pozgay S, Fishwick S (2010) Seismic tomography: a window into deep Earth. *Phys Earth Planet Inter* 178:101–135
- Ritsema J, van Heijst HJ, Woodhouse JH (1999) Complex shear wave velocity structure imaged beneath Africa and Iceland. *Science* 286:1925–1928
- Rost S, Garnero EJ (2006) Detection of an ultralow velocity zone at the core-mantle boundary using diffracted PKKP_{ab} waves. *J Geophys Res* 111:B07309
- Rost S, Revenaugh J (2003a) Small-scale ultralow-velocity zone structure imaged by ScP. *J Geophys Res* 108:2056
- Rost S, Revenaugh J (2003b) Detection of a D'' discontinuity in the south Atlantic using PKKP. *Geophys Res Lett* 30:1840
- Rost S, Thomas C (2002) Array seismology: methods and applications. *Rev Geophys* 40:1008
- Rost S, Garnero EJ, Stefan W (2010) Thin and intermittent ultralow-velocity zones. *J Geophys Res* 115:B06312
- Sacchi M, Ulrych TJ (1995) High-resolution velocity gathers and offset space reconstruction. *Geophysics* 60:1169–1177

- Sakai T, Kondo T, Ohtani E, Terasaki H, Endo N, Kuba T, Suzuki T, Kikegawa T (2006) Interaction between iron and post-perovskite at core-mantle boundary and core signature in plume source region. *Geophys Res Lett* 33:L15317
- Schultz R, Gu YJ (2013) Flexible, inversion-based Matlab implementation of the Radon transform. *Comput Geosci* 52:437–442
- Simmons NA, Forte AM, Boschi L, Grand SP (2010) GyPSuM: a joint tomographic model of mantle density and seismic wave speeds. *J Geophys Res* 115:B12310
- Sun D, Miller MS (2013) Study of the western edge of the African large low shear velocity province. *Geochem Geophys Geosyst* 14:3109–3125
- Sun D, Helmberger DV, Miller MS, Jackson JM (2016) Major disruption of D'' beneath Alaska. *J Geophys Res Solid Earth* 121:3534–3556
- Sylvander M, Ponce B, Souriau A (1997) Seismic velocities at the core-mantle boundary inferred from P waves diffracted around the core. *Phys Earth Planet Inter* 101:189–202
- Tackley PJ (2012) Dynamics and evolution of the deep mantle resulting from thermal, chemical, phase and melting effects. *Earth-Sci Rev* 110:1–25
- Thomas C, Weber M, Wicks CW, Scherbaum F (1999) Small scatterers in the lower mantle observed at German broadband arrays. *J Geophys Res* 104:15,073–15,088
- Thorne MS, Garnero EJ (2004) Inferences on ultralow-velocity zone structure from a global analysis of SPdKS waves. *J Geophys Res* 109:B08301
- Thorne MS, Garnero EJ, Grand S (2004) Geographic correlation between hot spots and deep mantle lateral shear-wave velocity gradients. *Phys Earth Planet Inter* 146:47–63
- Thorne MS, Garnero EJ, Jahnke G, Igel H, McNamara AK (2013) Mega ultra low velocity zone and mantle flow. *Earth Planet Sci Lett* 364:59–67
- Vidale JE, Hedlin MAH (1998) Evidence for partial melt at the core-mantle boundary north of Tonga from the strong scattering of seismic waves. *Nature* 391:682–685
- Voorhies CV (1986) Steady flows at the top of Earth's core derived from geomagnetic field models. *J Geophys Res* 91:12444–12446
- Wang Y, Wen L (2004) Mapping the geometry and geographic distribution of a very low velocity province at the base of the Earth's mantle. *J Geophys Res* 109:B10305
- Wang Y, Wen L (2007) Geometry and P and S velocity structure of the "African Anomaly". *J Geophys Res* 112:B05313
- Waszek L, Thomas C, Deuss A (2015) PKP precursor: implications for global scatterers. *Geophys Res Lett* 42:3829–3838
- Wentzcovitch RM, Tsuchiya T, Tsuchiya J (2006) MgSiO₃ postperovskite at D'' conditions. *Proc Natl Acad Sci USA* 103:543–546
- Wessel P, Smith WHF (1995) New version of the generic mapping tools released. *EOS Trans AGU* 76:329
- Wicks JK, Jackson JM, Sturhahn W (2010) Very low sound velocities in iron-rich (Mg, Fe)O: implications for the core-mantle boundary region. *Geophys Res Lett* 37:L15304
- Williams Q, Garnero EJ (1996) Seismic evidence for partial melt at the base of the Earth's mantle. *Science* 273:1528–1530
- Wyssession ME (1996) Large-scale structure at the core-mantle boundary from core-diffracted waves. *Nature* 382:244–248
- Wyssession ME, Okal EA (1989) Regional analysis of D'' velocities from the ray parameters of diffracted P profiles. *Geophys Res Lett* 16:1417–1420
- Wyssession ME, Okal EA, Bina CR (1992) The structure of the core-mantle boundary from diffracted waves. *J Geophys Res* 97:8749–8764
- Xu Y, Koper KD (2009) Detection of a ULVZ at the base of the mantle beneath the northwest Pacific. *Geophys Res Lett* 36:L17301
- Zhao D (2004) Global tomographic images of mantle plumes and subducting slabs: insight into deep Earth dynamics. *Phys Earth Planet Inter* 146:3–34

Submit your manuscript to a SpringerOpen[®] journal and benefit from:

- ▶ Convenient online submission
- ▶ Rigorous peer review
- ▶ Open access: articles freely available online
- ▶ High visibility within the field
- ▶ Retaining the copyright to your article

Submit your next manuscript at ▶ springeropen.com
